Title

Addition of Ianalumab (VAY736) to Ibrutinib in Patients with Chronic Lymphocytic Leukemia on Ibrutinib Therapy: Results from a Phase Ib Study.

Journal

Clinical Cancer Research, 31(24)

ISSN

1078-0432

Authors

Rogers, Kerry A
Yan, Pearlly
Flinn, Ian W
et al.

Publication Date

2025-12-15

DOI

10.1158/1078-0432.ccr-25-0210

Addition of Ianalumab (VAY736) to Ibrutinib in Patients with Chronic Lymphocytic Leukemia on Ibrutinib Therapy: Results from a Phase Ib Study

Kerry A. Rogers[1], Pearlly Yan[1,2], Ian W. Flinn[3], Deborah M. Stephens[4], Thomas J. Kipps[5], Sarah M. Larson[6], Laura Martz[1], Xi Chen[2], Huabao Wang[2], Ethan Hopping[2], Ralf Bundschuh[1,7,8], Altan Turkoglu[9,10], Gerard Lozanski[11], Carolyn McGarry[12], Alexandra Acosta[12], Romain Sechaud[13], Daniela Baldoni[13], Anwesha Chaudhury[14], Jeanne Whalen[15], Nadia B. Hassounah[15], Nina Orwitz[16], Javier Otero[12], Janghee Woo[12], and John C. Byrd[17]

ABSTRACT

Purpose: This phase Ib dose-escalation/expansion trial (NCT03400176) enrolled patients with CLL who did not achieve a complete response (CR) with ibrutinib or had developed resistance mutations. Ianalumab (VAY736), an anti–B cell–activating factor receptor monoclonal antibody, combined with ibrutinib significantly improved survival and reduced tumor burden in preclinical chronic lymphocytic leukemia (CLL) models.

Patients and Methods: Patients received intravenous ianalumab (escalation: 0.3–9.0 mg/kg; expansion: 3.0 mg/kg) once every 2 weeks and continued ibrutinib (420 mg) once daily for up to eight cycles of 28 days. The study aimed to evaluate the safety, tolerability, recommended dose, and antitumor activity of this combination.

Results: Thirty-nine patients were treated (escalation: $n = 15$; expansion: $n = 24$). No dose-limiting toxicities were observed. Of the 39 patients, 38.5% were in CR or CR with incomplete marrow recovery at cycle 9 (C9). At C9 day 1, 17 patients (43.6%) achieved undetectable measurable residual disease in blood or bone marrow. Grade ≥3 adverse events occurred in 16 patients (41.0%), which were treatment-related in nine (23.1%). No on-treatment deaths were reported; one patient died because of COVID-19 during the posttreatment period. Seventeen patients (43.6%) discontinued ibrutinib at or after C9 day 1 and remained off therapy for 12.1 to 24.5 months. Preliminary RNA sequencing and flow cytometry data support both NK- and T-cell activation with ianalumab.

Conclusions: The combination was well tolerated, with 43.6% of patients discontinuing ibrutinib therapy. Biomarker data suggest that ianalumab increased NK- and T-cell activation. These data support further evaluations of ianalumab in combination with Bruton tyrosine kinase inhibitors for patients with CLL.

Introduction

Bruton tyrosine kinase (BTK) is a nonreceptor tyrosine kinase involved in B-cell antigen receptor signaling in both normal and transformed B lymphocytes (1). The B-cell receptor signaling pathway is critical in chronic lymphocytic leukemia (CLL), as evidenced by the success of BTK inhibitors (BTKi) in the therapy for CLL. The first-in-class–approved BTKi (ibrutinib) and subsequent BTKi (acalabrutinib, zanubrutinib, and pirtobrutinib) have demonstrated dramatic impact on the outcomes (2, 3). However, BTKi therapy requires continuous, indefinite treatment, which may result in long-term toxicity, including cardiac toxicities such as atrial fibrillation, bleeding, and hypertension (4). In a real-world analysis trial of 616 patients treated with ibrutinib in the United States, 41% of patients had discontinued ibrutinib at a median follow-up of 17 months, with the main reason being toxicity, including arthralgia, atrial fibrillation, and rash (5). Moreover, patients treated with BTKi may develop resistance, leading to disease relapse or progression. In approximately 70% of patients developing resistance to BTKi, the resistance has been attributed to

[1]Division of Hematology, Department of Internal Medicine, The Ohio State University, Columbus, Ohio. [2]Genomics Shared Resource, The Ohio State University Comprehensive Cancer Center, Columbus, Ohio. [3]Tennessee Oncology and One Oncology, Nashville, Tennessee. [4]Lineberger Comprehensive Cancer Center at University of North Carolina, Chapel Hill, North Carolina. [5]UC San Diego, Moores Cancer Center, La Jolla, California. [6]Ronald Reagan UCLA Medical Center, Los Angeles, California. [7]Department of Physics, The Ohio State University, Columbus, Ohio. [8]Department of Chemistry and Biochemistry, The Ohio State University, Columbus, Ohio. [9]Department of Electrical & Computer Engineering, The Ohio State University, Columbus, Ohio. [10]The Ohio State University Comprehensive Cancer Center, James Cancer Hospital and Solove Research Institute, Columbus, Ohio. [11]Department of Pathology, The Ohio State University, Columbus, Ohio. [12]Biomedical Research, Novartis Pharmaceuticals Corporation, East Hanover, New Jersey. [13]Biomedical Research, Novartis Pharma AG, Basel, Switzerland. [14]Novartis Pharmaceuticals Corporation, Cambridge, Massachusetts. [15]Biomedical Research, Novartis Pharmaceuticals Corporation, Cambridge, Massachusetts. [16]Novartis Pharmaceuticals Corporation, East Hanover, New Jersey. [17]Department of Internal Medicine, University of Cincinnati, Cincinnati, Ohio.

Current address for J. Woo: Winship Cancer Institute, Emory University, Atlanta, Georgia.

Corresponding Authors: Kerry A. Rogers, Division of Hematology, Department of Internal Medicine, The Ohio State University, 410 West 12th Avenue, Suite 455, Columbus, OH 43210. E-mail: Kerry.Rogers@osumc.edu; and John C. Byrd, Department of Internal Medicine, University of Cincinnati, 231 Albert Sabin Way, Cincinnati, OH 45267-0551. E-mail: byrd2jc@ucmail.uc.edu

Clin Cancer Res 2025;31:5145–58

doi: 10.1158/1078-0432.CCR-25-0210

Translational Relevance

Chronic lymphocytic leukemia (CLL) is the most prevalent adult leukemia. A current standard of care for CLL includes indefinite treatment with Bruton tyrosine kinase inhibitors, such as ibrutinib, acalabrutinib, or zanubrutinib, which may result in long-term toxicity. In preclinical studies, ianalumab (VAY736), a human monoclonal antibody targeting B cell–activating factor receptor–positive B cells, showed antileukemic activity; when combined with ibrutinib, it significantly reduced tumor burden and improved survival in animal models. We conducted a phase Ib dose-escalation/expansion study of ianalumab with ibrutinib in 39 patients with CLL. The combination was well tolerated with an acceptable safety profile in patients with CLL. Seventeen patients (43.6%) attained a response with undetectable measurable residual disease in blood or marrow. Biomarker data suggested that ianalumab increased the activation of NK and T cells. These data provide evidence in favor of further studies investigating ianalumab in patients with CLL.

mutations in *BTK* at the C481 drug–binding site, other sites in the BTK protein, or the downstream effector phospholipase C gamma 2 (*PLCγ2*; refs. 1, 6–10).

Therapies combined with ibrutinib, such as rituximab, have shown prolongation of progression-free survival (PFS) and overall survival compared with standard chemoimmunotherapy. However, in a randomized phase III study for patients with untreated CLL that had both ibrutinib and ibrutinib + rituximab arms, there was no PFS benefit with the addition of rituximab (11). In contrast, the CD20 antibody, obinutuzumab, when added to acalabrutinib, improved complete response (CR) rate and PFS over acalabrutinib monotherapy in patients with previously untreated CLL (12). An update of this study also demonstrated that acalabrutinib and obinutuzumab demonstrated a prolongation of overall survival over chemoimmunotherapy, which was not observed with acalabrutinib alone. These data suggest that an Fc-engineered antibody with improved effector cell activation might impart the best opportunity for an antibody to be effective with a BTKi. However, the depth of response [e.g., CR or undetectable measurable residual disease (uMRD)] remains low in these combinations, and BKTi are generally dosed continuously, highlighting the need for investigating a mechanism for improving responses to discontinue BTKi (13, 14).

B cell–activating factor receptor (BAFF-R) is expressed on most B-cell receptor–positive B cells, and BAFF-R signaling has been shown to be involved in the activation, including proliferation, maturation, and survival, of normal and malignant B cells (15, 16). Furthermore, BAFF-R signaling plays a role in B cell–mediated human diseases such as autoimmune disorders and B-cell malignancies, and some polymorphisms in *BAFF*/*BAFF-R* genes have been associated with increased risk of developing CLL (17).

Ianalumab (VAY736) is a human monoclonal antibody targeting BAFF-R–positive B cells for elimination via antibody-dependent cell-mediated cytotoxicity (ADCC; ref. 18). Ianalumab has several mechanisms of action: (i) by blocking BAFF ligand from binding to BAFF-R, it blocks BAFF-R and downstream NF-κB signaling, which prevents B-cell differentiation, proliferation, and survival; (ii) by depletion of B cells by mediating potent ADCC through binding to both NK cells in the periphery and in the CLL tumor microenvironment; and (iii) by triggering macrophage antibody-dependent cellular phagocytosis of CLL cells (18, 19). Ianalumab has demonstrated antileukemia activity in preclinical CLL models that is significantly superior to that of anti-CD20 monoclonal antibodies, including rituximab and obinutuzumab, which specifically bind to B cell–specific cell surface antigen, CD20, and induce killing of normal and malignant B cells via ADCC (18). BAFF/BAFF-R interactions activate an alternative NF-κB–dependent survival signaling compared with the NF-κB signaling inhibited by BTKi such as ibrutinib (18, 20, 21), meaning that ianalumab can inhibit NF-κB synergistically with BTKi and targets a different antigen other than CD20. This led to the hypothesis that a combination of ibrutinib with the BAFF-R antibody, ianalumab, may improve the efficacy of ibrutinib treatment.

In *in vitro* models of human CLL cells and *in vivo* CLL mouse models, ianalumab demonstrated antileukemia activity that, when combined with ibrutinib, could significantly reduce tumor burden and improve the survival in the mouse leukemia model, suggesting that this combination may augment the antileukemia response. This potentially could allow patients to discontinue ibrutinib and reduce the toxicity related to continuous therapy (18). This article presents the results from the first phase Ib dose-escalation/expansion study of ianalumab in combination with ibrutinib in patients with CLL (NCT03400176).

Patients and Methods

Study design

This is a phase Ib, open-label, multicenter (from seven centers in the United States) dose-escalation and dose-expansion study evaluating the safety, tolerability, recommended dose for expansion (RDE), pharmacokinetics (PK), pharmacodynamics, and antitumor activity of the combination of ianalumab with ibrutinib in adult patients with CLL. Patients were enrolled from April 15, 2018, to April 12, 2022.

In the escalation part, patients received the standard, approved dose of oral ibrutinib (420 mg daily) in all cohorts. Ianalumab dosages of 0.3, 1.0, 3.0, and 9.0 mg/kg, given intravenously, once every 2 weeks, were tested in consecutive cohorts, supported by Bayesian analysis conducted ahead of each new dose cohort. The dosing cycle was 28 days. Ianalumab starting dosage of 0.3 mg/kg once every 2 weeks in patients with CLL was selected based on simulations of PK–B-cell dynamics using prior ianalumab data in immunology indications, along with adjustments to B-cell attributes and rate constants for patients with CLL (22, 23). An optimal dose of ianalumab 3.0 mg/kg in combination with ibrutinib was identified based on data and analysis gathered during the dose escalation.

In the expansion part, patients received ianalumab 3.0 mg/kg once every 2 weeks intravenously and were enrolled into two arms depending on whether they had ibrutinib resistance mutations present at enrollment (arm A, patients without ibrutinib resistance mutations and arm B, patients with ibrutinib resistance mutations in their CLL).

The on-treatment period was up to eight cycles of 28 days (C8D28). Patients received ianalumab in combination with ibrutinib (420 mg or highest tolerated dose, defined prior to study enrollment) for up to six cycles of 28 days. After six cycles, patients with a CR discontinued ianalumab and received ibrutinib for an additional two cycles; patients without a CR after six cycles continued to receive ianalumab + ibrutinib for the remaining two cycles. In the original protocol, patients achieving uMRD at cycle 9 day 1 (C9D1)

could discontinue ibrutinib at the investigator's discretion; this was amended so that the treatment decisions were based on clinical response following International Workshop on CLL (iwCLL) response criteria (patients with CR at C9D1 could discontinue ibrutinib; ref. 24).

Participants

The study recruited adult patients with CLL diagnosed as per World Health Organization classification of hematologic disorders or iwCLL guidelines (24, 25). Eligible patients had received ibrutinib either as first-line treatment (single agent or in combination) or following relapse from another approved treatment; patients had either not achieved a CR after more than 1 year of ibrutinib treatment or developed a known ibrutinib resistance mutation [mutations in *BTK* (*C481S*) and/or mutations in the immediate downstream target of BTK, *PLCγ2*; ref. 26]. Only the following *PLCγ2* mutations were considered functional mutations: R665, S707, A708, and L845. Patients had an Eastern Cooperative Oncology Group performance status of 0 to 2, and platelet levels of $\geq 25 \times 10^9$/L without transfusion support within 7 days of the first dose of ianalumab. Detailed inclusion and exclusion criteria are listed in Supplementary Methods. The overall representativeness of this study population to the general CLL population is shown in Supplementary Table S1.

In the dose-escalation part, patients who had been receiving ibrutinib 420 mg following relapse on another approved therapy and meeting the criteria for nonresponse or ibrutinib resistance mutations (*BTK* or *PLCγ2*) were included.

In the dose-expansion part, patients who had received ibrutinib at a dose <420 mg and whose response had been stable on that dose for 2 months prior to trial treatment were also included. The expansion part consisted of the following two arms: the first arm (arm A) included patients who had received ibrutinib either following relapse from another approved therapy or as first-line therapy (alone or in combination) and who had not achieved CR after 1 year, and the second arm (arm B) included patients who had developed ibrutinib resistance mutations after relapse or first-line therapy (alone or in combination).

Patients who received live vaccine within 4 weeks of starting ianalumab and those with a known history of human immunodeficiency virus or with active hepatitis B or C infection were excluded from the study.

Procedures

Outcomes

For the escalation part, the safety primary endpoints were dose-limiting toxicities (DLT) and were reported within the first 28 days of treatment with ianalumab in combination with ibrutinib. For both escalation and expansion parts, the safety primary endpoints were the incidence and severity of adverse events (AE) and serious AEs. The tolerability primary endpoints included dose interruptions, reduction, and dose intensity (computed as the ratio of actual cumulative dose received and actual duration of exposure).

The key secondary endpoints were the rate of CR/CR with incomplete marrow recovery (CRi) at the beginning of C9 (C9D1), overall response rate (ORR) assessed by iwCLL criteria (24), and clearance of ibrutinib resistance mutations (BTK^{C481S} and/or *PLCγ2* hotspot) defined as less than 1% mutation-bearing alleles for the patients in the arm with ibrutinib resistance mutations at baseline. Mutation testing was performed using peripheral blood (and some bone marrow aspirate) samples for $CD19^+$ leukocytes using RoboSep-S (EasySep HLA Chimerism Whole Blood CD19 Positive Kit, STEMCELL Technologies). Samples collected at C1D1, cycle 4 day 1, cycle 7 day 1, C9D1, and after C9D1 were further assessed every 3 months for 2 years of follow-up for patients with CR, partial response (PR), or whose disease was assessed as stable disease (SD) at C9D1. Next-generation sequencing for the coding region of BTK^{C481S} and *PLCγ2* was performed on all baseline samples using a fully validated custom AmpliSeq assay on the Ion Torrent S5 platform (Thermo Fisher Scientific) at the Clinical Laboratory Improvement Amendments–certified Ohio State University's James Molecular Laboratory, with bioinformatic analysis incorporating Ion Torrent suite tools, GenomOncology Workbench,, and review of low-level variants in the Integrative Genomics Viewer (Broad Institute). The sensitivity of mutation detection was 0.5% variant allele fraction (VAF) for BTK^{C481S} and *PLCγ2* hotspot resistance–associated mutations (27). Subsequent samples from patients with *PLCγ2* mutations were analyzed using NGS. For monitoring of patients with BTK^{C481S} mutation, BTK^{C481S}-specific quantitative Droplet Digital PCR was performed on the QX200 Droplet Digital PCR System (Bio-Rad Laboratories) using a custom assay performed in the same Clinical Laboratory Improvement Amendments laboratory. Analysis and quantitation of Droplet Digital PCR data were performed using QX Manager software (Bio-Rad Laboratories). A positive mutation result was reported at or above the validated sensitivity of 0.1% mutation proportion if at least five mutant events were observed. Separate probes recognizing the two common BTK^{C481S} changes, c.1442G>C and the c.1441G>A, were included, as well as a wild-type probe at that location with the percentage of mutant to total BTK^{C481S} events reported. Alternate droplet patterns, possibly indicative of other BTK p.C481X sequence changes, were further investigated using the BTK^{C481S}–*PLCγ2* sequencing assay.

Biomarker analyses

MRD in blood and bone marrow was assessed using 10-color multiparametric flow cytometry analysis (28, 29). The following markers were used for the MRD assessment using flow cytometry with a three-tube panel: CD2, CD3, CD5, CD7, CD9, CD10, CD13, CD14, CD19, CD20, CD22, CD38, CD43, CD45, CD56/16, CD79b, CD81, FMC-7, HLA DR, kappa, and lambda. MRD in bone marrow was assessed at screening and at C9D1. MRD in blood was assessed at screening, C1D1, cycle 1 day 2, cycle 1 day 8, cycle 1 day 15, cycle 2 day 1, cycle 3 day 1, cycle 4 day 1, cycle 5 day 1, cycle 6 day 15, and C9D1, and for patients who continued to take ianalumab treatment, it was assessed at cycle 7 day 1 and cycle 8 day 1. After C9D1, MRD was assessed every 3 months for 2 years for patients with CR, PR, or SD at C9D1. Patients were defined as having uMRD if they had blood or marrow with <1 CLL cell per 10,000 leukocytes.

Samples of human peripheral blood mononuclear cells (PBMC) were collected for NK-cell biomarker assessment by flow cytometry at C1D1 before the first dose of ianalumab treatment, 1 hour and 20 to 24 hours after the first dose, and at C9D1. PBMCs were cryopreserved and later stained for flow cytometry analysis. Briefly, up to 4×10^6 cryopreserved PBMCs were thawed quickly in a water bath at 37°C and washed by centrifugation with prewarmed RPMI medium containing 10% of FBS. After washing, cells were stained with fixable viability dye eFluor 506 (Thermo Fisher Scientific) at a dilution of 1:100 in wash buffer (PBS containing 0.1% sodium azide and 2% FBS), followed by staining with fluorochrome-conjugated surface antibodies for 30 minutes at room temperature in the dark.

Previously prepared and qualified antibody cocktails consisting of 12 surface antibodies were utilized. The list of antibodies used for this panel is provided in Supplementary Table S2 (30).

After incubation, cells were washed once by centrifugation in wash buffer and fixed with 1× Fixation/Permeabilization Buffer from the Foxp3/Transcription Factor Staining Buffer Set (Thermo Fisher Scientific) for 30 minutes at room temperature in the dark. After fixation, cells were washed once by centrifugation with 1× Permeabilization Buffer from the Foxp3/Transcription Factor Staining Buffer Set and resuspended in 1× Permeabilization Buffer. Fluorochrome-conjugated intracellular antibody (Ki67) was added, and cells were incubated for 30 minutes at room temperature in the dark. Cells were then washed twice by centrifugation with 1× Permeabilization Buffer and resuspended in 0.5% formalin solution.

Cells were then acquired on a BD LSRFortessa X-20 equipped with five lasers (BD Biosciences), and data were analyzed using FlowJo software (FlowJo LLC; RRID: SCR_008520). For data analysis of the NK-cell proliferation assay, after exclusion of debris, doublets, and dead cells, NK cells were further gated for NK subsets (CD56, and CD16) as well as inhibition (CD159a) and activation [CD25, CD335, and NK group 2D (NKG2D)] biomarkers. Monocytes were also assessed for CD14, CD16, and HLA-DR expression. Samples of PBMCs were collected for gene expression analysis of CLL cell and immune cell signaling at C1D1 before the first dose of ianalumab treatment and 1 hour and 20 to 24 hours after the first dose. Two PBMC batches were isolated and kept separately for analysis. PBMC isolation occurred at the clinical site for batch 1 and at the central lab for batch 2. PBMCs were cryopreserved and later sorted into $CD4^+$ T cells, $CD8^+$ T cells, $CD56^+$ NK cells, and $CD19^+CD5^+$ CLL cells for *in situ* ultralow input full-length complementary DNA generation, followed by transcriptome library generation and sequencing [coverage-based limiting-cell experimental analysis for RNA sequencing (CLEAR)]. For cell-based limiting-cell RNA sequencing (RNA-seq), cryopreserved patient PBMC samples from three time points (predrug dose, 1 hour after dose, and 20–24 hours after dose) were quickly thawed in a water bath at 37°C. Cells were gently dispersed in 10 mL of media and then centrifuged at 1,000 rpm for 10 minutes at 4°C. The supernatant was aspirated off, and cell pellets were resuspended in media for enumeration; then, cells were resuspended with sterile PBS for antibody staining.

CD3, CD4, CD5, CD8, CD16, CD19, and CD56 antibodies were purchased from BD Pharmingen (PE-Cy7 Mouse Anti–Human CD3, cat. #557749, RRID: AB_396855; FITC Mouse Anti–Human CD4, cat. #555346, RRID: AB_395751; APC-Cy7 Mouse Anti–Human CD5, cat. #563516, RRID: AB_2738249; BV510 Mouse Anti–Human CD8, cat. #563256, RRID: AB_2738101; APC Mouse Anti–Human CD16, cat. #561304, RRID: AB_10714780; PE Mouse Anti–Human CD19, cat. #555413, RRID: AB_395813; and PerCP-Cy5.5 Mouse Anti–Human CD 56, cat. #560842, RRID: AB_2033964). PBMCs were stained as shown in Supplementary Table S3. A portion of the cells, up to 1 million, was kept as unstained control. Healthy donor PBMCs that were obtained and cryopreserved were used across days as a staining control. Antibody-binding beads from Invitrogen (UltraComp eBeads Plus Compensation Beads, reference #01-3333-42) were used for single-color compensation controls (Supplementary Table S4).

Stained cells were briefly vortexed and incubated in the dark on ice for 30 minutes. Tubes were washed with 2 mL FACS buffer and then spun down at 1,000 rpm for 10 minutes. After removal of the supernatant, the cells were resuspended with sterile PBS in final volumes of 500 μL and beads in 200 μL. They were stored on ice in the dark until FACS sorting.

For *in situ* cDNA generation, library preparation, sequencing, and data analysis, the Clontech SMART-Seq HT (Takara Bio, cat. #634437) kit was used for global cDNA generation. Cells (300 cells for most samples; 50–250 cells for a few patient cell types) were sorted directly into freshly diluted SMART-Seq HT CDS Sorting Solution (lysis component: Takara Bio, cat. #634439; RNase inhibitor: Takara Bio, cat. #2313A). cDNA generation followed the manufacturer's manual, except the reagents were miniaturized to one fifth of the protocol volume for all enriched cell lysates. The quality (majority of cDNAs between 7 and 10 kb) and the quantity of purified cDNAs were assessed prior to sequencing library generation using the Agilent Bioanalyzer HS DNA kit and the Invitrogen Qubit DNA HS Assay kit. Sequencing libraries were generated using the Illumina Nextera XT Kit and Nextera XT Index Kit v2 Set A following the manufacturer's instructions, except for the miniaturization of reagent volume to a quarter of the listed volume. Purified library products were sequenced on Illumina NovaSeq 6000 flow cells using paired-end 100 bp to a depth of 17 to 20 million clusters. FASTQ files generated for each library were trimmed using AdapterRemoval v2.2.0, (RRID: SCR_011834; ref. 31), ensuring that all sequencing adapters were removed and that the average quality score for each read was above Q20 (representing 1 in 100 Illumina base error rate). Reads, which were aligned by HISAT2 v2.2.1, (RRID: SCR_015530; ref. 32) against rRNAs, mitochondrial DNAs, or PhiX bacteriophage (Illumina spike-in control) sequences, retrieved from NCBI (RefSeq Human Release 109.20210514, RRID: SCR_003496; ref. 33), were removed from each FASTQ file, as these do not represent gene expression signal of interest. All remaining reads were aligned against the reference human genome GRCh38p7 with HISAT2. The resulting BAM alignment files were sorted and indexed before further analysis.

Alignments were quantified using the featureCounts utility from the Subread package (v2.0.3, RRID: SCR_012919; refs. 34, 35) in unstranded mode using NCBI RefSeq human genes (see above) in GTF format. Custom Python scripts were used to produce a formatted gene expression counts table from the raw output of featureCounts. RNA-seq quality metrics were derived using a modification of the QuaCRS quality control workflow (36), which includes running RNA-SeQC (v1.1.8.1, RRID: SCR_005120; ref. 37), FASTQC (v0.11.5, RRID: SCR_014583), and RSeQC (v2.6.2, RRID: SCR_005275; ref. 38). Finally, coverage maps of each BAM file were derived using the bedtools "genomecov" utility (v2.28.0, RRID: SCR_006646; ref. 39).

RNA-seq coverage maps were preprocessed with the CLEAR (v1.0, RRID: SCR_027171; ref. 40) workflow to determine which genes were reliably quantified. In brief, read coverage distributions were profiled by CLEAR in a gene-by-gene manner. Per sample read coverage with a profile deviating from a double beta distribution was deemed "non-CLEAR passed" and therefore not used in downstream time point analysis. The final counts table consisted of raw gene read counts for all RefSeq genes or "not applicable" was added to replace read counts for "non-CLEAR passed" genes.

The following genes have been assessed for NK- and T-cell activation: *ETS1*, *KLRD1*, *ISG20*, and *PRF1* in NK cells; *ETS1*, *CD53*, *ISG20*, and *PRF1* in $CD8^+$ T cells; and *ADAM10*, *BIRC3*, *ITK*, and *CASP6* in $CD4^+$ T cells. The apoptosis-related gene signature included *BCL2*, *BIRC2*, *BIRC3*, *CASP3*, *CASP8*, *CFLAR*, *CYCS*, *NFKBIA*, *RELA*, and *TNFRSF10A* genes.

Gene expression analysis was completed for each cell type population separately. The raw read counts were trimmed mean of M-values normalized using the R package edgeR (v3.26.8, RRID: SCR_012802). Batch 1 and batch 2 datasets were combined, but colored differently, to increase sample numbers. Only patients with paired 0-hour pre-dose and 1-hour post-dose CLEAR-passed samples were included for each gene.

PK and BAFF-R occupancy

Pre-dose and post-dose blood samples for ianalumab PK, immunogenicity (anti-ianalumab antibodies), soluble BAFF, and BAFF-R occupancy (RO) were collected during ianalumab treatment. A detailed sampling schedule is provided in Supplementary Table S5. These included full PK profile for ianalumab at C1 and cycle 3 day 1 to day 15 and immunogenicity at C1D1, cycle 1 day 15, and day 1 of cycle 2 to cycle 8 (cycle 7 and cycle 8 if applicable). Blood samples were also collected for PK analysis of ibrutinib at C1D1 and cycle 1 day 8 at the following time points: before dose; 0.5, 2, 6, and 24 hours (cycle 1 only) after dose; and before dose on day 1 of cycle 2 to cycle 8. Ianalumab and soluble BAFF concentrations in serum were measured using a validated sandwich ELISA assay, with lower limit of quantification of 0.025 μg/mL and 62.5 pg/mL, respectively. BAFF-RO assay was a validated flow cytometry assay in whole blood. Ibrutinib concentrations in plasma were derived using a validated LC/MS assay, with a lower limit of quantification of 0.5 ng/mL. The presence of antidrug antibodies (ADA) in clinical study samples was evaluated using a validated assay in a three-tiered approach using a bridging format electrochemiluminescence assay.

Statistical and PK analyses

In the escalation phase, the protocol-specified MTD was defined as the highest combination dose with an estimated DLT rate below 33% in the first cycle of treatment. The Bayesian logistic regression model provided an estimate of ianalumab and ibrutinib combination not exceeding the MTD, which is typically the highest combination with less than 25% risk of excessive toxicity. The RDE was defined as a dose less than or equal to MTD, with the most appropriate benefit–risk assessment according to the investigators/sponsor, based on the safety and tolerability, PK, and pharmacodynamic data. The full analysis set consisted of all patients who received at least one dose of study treatment.

The dose-determining set included all patients from the full analysis set who met the minimum exposure criterion of taking the planned doses of ianalumab for the first 28 days and 75% of the planned ibrutinib doses, had sufficient safety evaluations, or experienced a DLT during cycle 1 (in the first 28 days of dosing). PK analysis set included all patients who provided an evaluable PK profile, which was considered as the following conditions being satisfied: the patient had received one of the planned treatments, provided at least one primary PK parameter, and did not vomit within 4 hours after ibrutinib dosing. PK parameters of ianalumab and ibrutinib were derived with WinNonlin Phoenix version 8.3.4 (Certara). PK parameters of ianalumab included total systemic exposure during the dosing interval (AUCtau), peak serum concentration (Cmax), time of maximum concentration observed, and elimination half-life.

The dose proportionality of ianalumab over the dose range of 0.3 to 9.0 mg/kg at cycle 1 and cycle 3 was evaluated by fitting a power model.

Descriptive summary statistics were used for summarizing continuous data, and frequencies and percentages were used for categorical data. ORR and their exact 90% confidence intervals (CI) were calculated based on a binomial distribution. Time to progression (TTP) is the time from the start of study treatment to the date of event which is defined as the first documented progression [defined as overall disease response assessment of progressive disease (PD)] or death due to underlying cancer. If a patient has not had an event, TTP is censored at the date of last adequate disease assessment. Assessments taken after the start of alternative cancer therapy will be excluded. TTP was estimated using the Kaplan–Meier method.

Ethical oversight

This study was conducted in accordance with the International Council for Harmonization of Technical Requirements for Registration of Pharmaceuticals for Human Use Harmonized Tripartite Guidelines for Good Clinical Practice, with applicable local regulations, including European Directive 2001/20/EC and US Code of Federal Regulations Title 21, and the Declaration of Helsinki. The protocol and all amendments were reviewed and approved by a properly constituted Institutional Review Board/Independent Ethics Committee/Research Ethics Board before study start. Eligible patients provided written, Institutional Review Board/Independent Ethics Committee/Research Ethics Board–approved informed consent prior to study start.

Results

Patient characteristics and disposition

A total of 39 patients were enrolled in the escalation part ($n = 15$) and the expansion part ($n = 24$), with expansion consisting of arm A for patients without ibrutinib resistance mutations ($n = 19$) and arm B for patients with ibrutinib resistance mutations in their CLL ($n = 5$).

Baseline patient demographics and characteristics are shown in **Table 1**. The median age was 65 years, and 92.3% of patients had an Eastern Cooperative Oncology Group performance status of 0. Twelve patients (30.8%), all of whom were enrolled in the ianalumab 3.0 mg/kg + 420 mg ibrutinib expansion part, had no prior therapies aside from ibrutinib before enrollment, and the median (min−max) number of prior therapies aside from ibrutinib was 1 (0–14). Of the enrolled patients, eight patients (20.5%) had BTK^{C481S} mutations, four (10.3%) had *PLCγ2* mutations, and three (7.7%) had both BTK^{C481S} and *PLCγ2* mutations. In terms of baseline CLL characteristics, six patients (15.4%) had 17p deletion, 32 patients (82.1%) had unmutated Ig heavy chain variable region genes, and 20 patients (51.3%) had a complex karyotype (≥5 abnormalities). At screening, as assessed by CT scans, 19 patients had one or more measurable lymph nodes present for which the sum of the product of perpendicular diameters of up to six lymph nodes was derived. The median sum of the product of perpendicular diameters was 464.0 mm^2, with a range of 0 to 4,343 mm^2. The absolute lymphocyte count at baseline was median (range) 5.45 (0.47–202.16) $\times 10^9$/L; 21 patients had absolute lymphocyte count >5 $\times 10^9$/L.

The median duration of exposure to ianalumab was 5.52 months (range, 1.8–7.8 months), and 53.8% of patients (21 of 39) had exposure between 5 and <6 months. During this trial, the median duration of exposure to ibrutinib was 7.39 months (range, 1.8–8.5 months), and 74.4% of patients (29 of 39) had exposure between 7 and <8 months during the on-treatment period.

Table 1. Patient baseline characteristics.

Demographic variable	Ianalumab 0.3 mg/kg + ibrutinib (420 mg) *N* = 4	Ianalumab 1.0 mg/kg + ibrutinib (420 mg) *N* = 3	Ianalumab 3.0 mg/kg + ibrutinib (280 mg) *N* = 1	Ianalumab 3.0 mg/kg + ibrutinib (420 mg) *N* = 27	Ianalumab 9.0 mg/kg + ibrutinib (420 mg) *N* = 4	All patients *N* = 39
Median age, years (range)	70.5 (61–75)	60.0 (60–63)	57.0 (57–57)	66.0 (39–82)	63.5 (54–79)	65.0 (39–82)
Sex, *n* (%)						
Male	4 (100)	2 (66.7)	1 (100)	20 (74.1)	1 (25.0)	28 (71.8)
Race, *n* (%)						
White	4 (100)	2 (66.7)	1 (100)	26 (96.3)	3 (75.0)	36 (92.3)
Black or African American	0	1 (33.3)	0	0	1 (25.0)	2 (5.1)
Missing	0	0	0	1 (3.7)	0	1 (2.6)
ECOG performance status, *n* (%)						
0	3 (75.0)	3 (100)	1 (100)	25 (92.6)	4 (100)	36 (92.3)
1	1 (25.0)	0	0	2 (7.4)	0	3 (7.7)
Prior antineoplastic regimens, *n* (%)						
Yes	4 (100)	3 (100)	1 (100)	27 (100)	4 (100)	39 (100)
Prior ibrutinib status, *n* (%)						
Only ibrutinib	0	0	0	12 (44.4)	0	12 (30.8)
At least one prior therapy and ibrutinib	4 (100)	3 (100)	1 (100)	15 (55.6)	4 (100)	27 (69.2)
Number of prior regimens excluding ibrutinib						
Median (range)	2.5 (1–4)	1.0 (1–2)	3.0 (3–3)	1.0 (0–6)	4.0 (2–14)	1.0 (0–14)
Baseline ibrutinib resistance mutation status—any mutation,[a] *n* (%)	1 (25.0)	3 (100)	1 (100)	7 (25.9)	3 (75.0)	15 (38.5)
BTK^{C481S}	1 (25.0)	2 (66.7)	0	4 (14.8)	1 (25.0)	8 (20.5)
PLCγ2	0	0	1 (100)	2 (7.4)	1 (25.0)	4 (10.3)
L845	0	0	1 (100)	0	1 (25.0)	2 (5.1)
D334	0	0	0	0	0	0
D1140	0	0	0	0	0	0
R665	0	0	0	3 (11.1)	1 (25.0)	4 (10.3)
S707	0	1 (33.3)	0	1 (3.7)	0	2 (5.1)
BTK^{C481S} + *PLCγ2*	0	1 (33.3)	0	1 (3.7)	1 (25.0)	3 (7.7)
Other	0	1 (33.3)	0	2 (7.4)	0	3 (7.7)
Dohner classification[b]						
Chromosome 17p deletion	0	2 (66.7)	0	3 (11.1)	1 (25.0)	6 (15.4)
Chromosome 11q deletion	1 (25.0)	0	0	6 (22.2)	2 (50.0)	9 (23.1)
Trisomy 12	0	1 (33.3)	0	2 (7.4)	0	3 (7.7)
Chromosome 13q deletion	3 (75.0)	0	0	7 (25.9)	0	10 (25.6)
None	0	0	1 (100)	9 (33.3)	1 (25.0)	11 (28.2)
IGHV-mutational status						
Mutated	1 (25.0)	0	0	5 (18.5)	0	6 (15.4)
Unmutated	2 (50.0)	3 (100)	1 (100)	22 (81.4)	4 (100)	32 (82.1)
Missing	1 (25.0)	0	0	0	0	1 (2.6)
Complex karyotype						
Yes	3 (75.0)	3 (100)	0	11 (40.7)	3 (75.0)	20 (51.3)
Absolute lymphocyte count (10^9/L) at screening						
Median (range)	8.31 (1.56–11.3)	37.28 (1.56–202.16)	0.47 (0.47–0.47)	5.28 (1.1–60.1)	15.02 (1.02–74.65)	5.45 (0.47–202.16)
SPD at screening (mm^2), *n*	2	2	1	12	2	19
Median (range)	541.5 (222–861)	500.0 (476–524)	2,290.0 (2,290–2,290)	272.0 (0–4,343)	1,026.5 (4–2,049)	464.0 (0–4,343)
Time from the start of ibrutinib therapy to the first study treatment (months), median (range)	20.76 (2.0–63.0)	49.58 (14.9–66.3)	7.43 (7.4–7.4)	24.97 (6.6–67.2)	64.44 (23.0–100)	24.97 (2.0–100)

Abbreviations: ECOG, Eastern Cooperative Oncology Group; IGHV, Ig heavy chain variable; SPD, sum of product of diameters.

[a]The ibrutinib resistance mutations measured in *BTK*^{C481S} and *PLCy2* are not mutually exclusive. *BTK*^{C481S} and *PLCγ2* (any variant) genetic mutations were assessed per patient. Patients with multiple specific classifications, or multiple *PLCγ2* variants, are counted in all corresponding rows. Other mutations include CD79A and M1141K. Patients with other mutations also had *PLCγ2*.

[b]The Dohner classification categories are defined as follows: patients with a 17p deletion; patients with an 11q deletion without a 17p deletion; patients with trisomy 12 without a 17p deletion, or an 11q deletion; patients with a 13q deletion without a 17p deletion, trisomy 12, or an 11q deletion; and patients with none of the four abnormalities.

Completion of ianalumab treatment was defined as reaching cycle 6 day 28 (C6D28), and completion of ibrutinib treatment was defined as reaching C8D28. Overall, 32 patients (82.0%) reached C6D28, seven patients (18.0%) discontinued ianalumab before C6D28, and the primary reason for ianalumab discontinuation was PD (10.3%, four of 39). Three other patients discontinued ianalumab early because of an AE (elevated

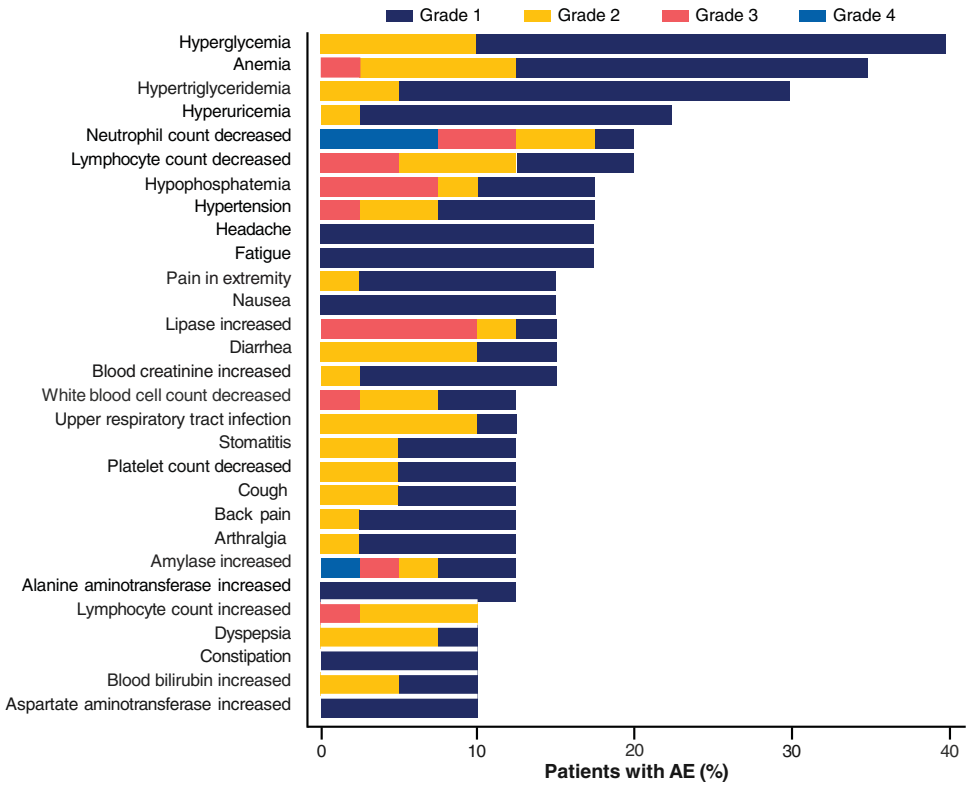

Figure 1.
AEs in the dose-escalation and -expansion phases of the study, regardless of cause or ianalumab dose, in ≥10% of patients.

amylase), subject decision, and physician decision. Thirty patients (76.9%) received ibrutinib until C8D28, with nine patients (23.1%) discontinuing ibrutinib primarily because of PD (12.8%, five of 39). Eleven patients (28.2%) were treated with ianalumab after C6D28 for an additional two cycles; 10 of these patients completed the full two cycles, and one patient (2.6%, one of 39) discontinued ianalumab because of physician's decision.

Safety

No DLTs were observed up to the highest tested ianalumab dosage of 9.0 mg/kg once every 2 weeks. AEs of any grade were reported in all patients (**Fig. 1**; **Table 2**). Hyperglycemia, any grade, was reported in 16 patients (41.0%), which occurred exclusively in the first cycle, did not require intervention, and was considered to be due to premedication with steroid (100 mg prednisolone or equivalent was recommended per protocol based on institutional guidelines). Grade ≥3 AEs were reported in 16 patients (41.0%), with the most common being neutropenia/decrease in neutrophil count (15.4%), followed by an increase in lipase (10.3%), hypophosphatemia (7.7%), decrease in lymphocyte count (5.1%), and amylase increase (5.1%). Two patients treated with ianalumab 3.0 mg/kg once every 2 weeks + ibrutinib 420 mg experienced grade ≤2 infusion-related reactions.

There was no observed relationship between the dosage of ianalumab and the occurrence of AEs. One patient in arm B of the expansion phase discontinued treatment because of a grade 4 AE, asymptomatic amylase increase (suspected to be treatment related). The amylase level normalized 15 days from the start date of the AE.

Serious AEs were reported in two patients. One patient in the ianalumab 3.0 mg/kg + ibrutinib 420 mg group reported grade 4 neutropenia/decrease in neutrophil count (suspected to be treatment related) and grade 3 noncardiac chest pain (not suspected to be treatment related), and another patient in the ianalumab 1.0 mg/kg + ibrutinib 420 mg group reported grade 4 neutropenia/decrease in neutrophil count (suspected to be treatment related). All patients with neutropenia or decreased neutrophil count were able to continue receiving treatment and did not experience neutropenia recurrence (of note, per protocol, the use of growth factors such as G-CSF was permitted according to institutional guidelines). Only three patients received this treatment while on the study). No on-treatment deaths were reported during the study. One patient died because of COVID-19 during the posttreatment period. The patient died more than a year after completing the ianalumab treatment while still on treatment with ibrutinib.

Any-grade infections and infestations (reported using Medical Dictionary for Regulatory Activities version 25 system organ class) were reported in 18 patients (46.2%), and there were no grade ≥3 infections reported during the on-treatment period.

Efficacy

Efficacy was assessed in 39 evaluable patients from the dose-escalation and -expansion parts. The ORR during dose escalation and expansion is shown in **Tables 3** and **4**. The ORR during the dose-escalation phase was 40% (90% CI, 19.1%–64%). Among the 15 patients assessed in escalation, six (40%) achieved CR, six (40%) achieved SD, and six (20%) had PD. The ORR during the dose-expansion phase was 70.8% (90% CI, 52.1%–85.4%). Among the 24 patients assessed in the expansion phase, eight (33.3%) achieved CR, eight (33.3%) achieved PR, and six (25%) achieved SD. Overall response at C9D1 (or before discontinuation) was 59% for all patients. Responses at C9D1 are shown for all patients in **Fig. 2A**

Table 2. AEs, regardless of study drug relationship, in dose-escalation and -expansion phases.

AE	Ianalumab 0.3 mg/kg once every 2 weeks + ibrutinib 420 mg *N* = 4	Ianalumab 1.0 mg/kg once every 2 weeks + ibrutinib 420 mg *N* = 3	Ianalumab 3.0 mg/kg once every 2 weeks + ibrutinib 280 mg *N* = 1	Ianalumab 3.0 mg/kg once every 2 weeks + ibrutinib 420 mg *N* = 27	Ianalumab 9.0 mg/kg once every 2 weeks + ibrutinib 420 mg *N* = 4	All patients *N* = 39
Patients with at least one event, any grade, *n* (%)	4 (100)	3 (100)	1 (100)	27 (100)	4 (100)	39 (100)
Treatment related, *n* (%)	2 (50.0)	2 (66.7)	1 (100)	15 (55.6)	1 (25.0)	21 (53.8)
Patients with at least one event, grade ≥3, *n* (%)	1 (25.0)	2 (66.7)	1 (100)	12 (44.4)	0	16 (41.0)
Treatment related, *n* (%)	0	1 (33.3)	1 (100)	7 (25.9)	0	9 (23.1)
Most common grade ≥3 AEs, *n* (%)[a]						
Neutropenia/ neutrophil count decreased	0	2 (66.7)	1 (100)	3 (11.1)	0	6 (15.4)
Lymphocyte count decreased	0	0	0	2 (7.4)	0	2 (5.1)
Anemia	0	0	0	1 (3.7)	0	1 (2.6)
Hypophosphatemia	0	1 (33.3)	0	2 (7.4)	0	3 (7.7)
Lipase increased	0	0	0	4 (14.8)	0	4 (10.3)
Leukocytosis	0	1 (33.3)	0	0	0	1 (2.6)
Noncardiac chest pain	0	0	0	1 (3.7)	0	1 (2.6)
White blood cell count decreased	0	1 (33.3)	0	0	1	1 (2.6)
Lymphocyte count increased	1 (25.0)	0	0	0	0	1 (2.6)
Amylase increased	0	0	0	2 (7.4)	0	2 (5.1)
Hypokalemia	0	0	0	1 (3.7)	0	1 (2.6)
Hypermagnesemia	0	1 (33.3)	0	0	0	1 (2.6)
Hypertension	0	0	0	1 (3.7)	0	1 (2.6)
Aortic aneurysm	0	0	0	1 (3.7)	0	1 (2.6)

[a]A patient may experience multiple AEs.

and by study part in **Fig. 2B** and are summarized by prior therapy (ibrutinib only vs. at least one therapy and ibrutinib) in Supplementary Table S6.

In the expansion phase (ianalumab 3.0 mg/kg + ibrutinib), the CR/CRi response rate at C9D1 was 37.5% (90% CI, 21.2–56.3), with CR achieved in eight patients (33.3%), CRi in one patient (4.2%), PR in six patients (25%), and SD in three patients (12.5%). Nine patients (47.4%, nine of 19) in expansion arm A achieved CR/CRi, and none of the expansion patients with a baseline ibrutinib resistance mutation (arm B) achieved a CR/CRi (Supplementary Table S7).

Seventeen patients (43.6%) elected to discontinue ibrutinib at or after C9D1 following CR and/or uMRD and, during the 2-year follow-up period, were able to remain off therapy between 12.1 and 24.5 months.

During dose escalation, 11 patients (73.3%) progressed, and the median TTP was 19.4 months (95% CI, 2.8–25.1). Four patients (26.7%) with no progression were censored at the date of the last adequate assessment. The Kaplan–Meier–estimated TTP rates at 6 and 12 months were 71.8% (95% CI, 41.1–88.4) and 64.6% (95% CI, 34.7–83.5), respectively. During dose expansion, four (16.7%)

Table 3. ORR. Best overall response in dose-escalation phase and all patients.

	Ianalumab 0.3 mg/kg once every 2 weeks + ibrutinib 420 mg *N* = 4 *n* (%)	Ianalumab 1.0 mg/kg once every 2 weeks + ibrutinib 420 mg *N* = 3 *n* (%)	Ianalumab 3.0 mg/kg once every 2 weeks + ibrutinib 420 mg *N* = 4 *n* (%)	Ianalumab 9.0 mg/kg once every 2 weeks + ibrutinib 420 mg *N* = 4 *n* (%)	All patients in dose escalation *N* = 15 *n* (%)	All patients *N* = 39 *n* (%)
Best overall response						
CR	2 (50.0)	0	2 (50.0)	2 (50.0)	6 (40.0)	14 (35.9)
CRi	0	0	0	0	0	1 (2.6)
PR	0	0	0	0	0	8 (20.5)
SD	1 (25.0)	2 (66.7)	2 (50.0)	1 (25.0)	6 (40.0)	12 (30.8)
PD	1 (25.0)	1 (33.3)	0	1 (25.0)	3 (20.0)	4 (10.3)
ORR (CR, CRi, or PR)	2 (50.0)	0	2 (50.0)	2 (50.0)	6 (40.0)	23 (59.0)
90% CI	(9.8–90.2)	(0–63.2)	(9.8–90.2)	(9.8–90.2)	(19.1–64.0)	(44.6–72.3)

Table 4. ORR. Best overall response in dose-expansion phase and all patients.

	Ianalumab 3.0 mg/kg once every 2 weeks arm A + ibrutinib 420 mg *N* = 19 *n* (%)	Ianalumab 3.0 mg/kg once every 2 weeks arm B + ibrutinib 280 mg *N* = 1 *n* (%)	Ianalumab 3.0 mg/kg once every 2 weeks arm B + ibrutinib 420 mg *N* = 4 *n* (%)	All patients in dose expansion N = 24 *n* (%)	All patients *N* = 39 *n* (%)
Best overall response					
CR	8 (42.1)	0	0	8 (33.3)	14 (35.9)
CRi	1 (5.3)	0	0	1 (4.2)	1 (2.6)
PR	7 (36.8)	0	1 (25.0)	8 (33.3)	8 (20.5)
SD	3 (15.8)	0	3 (75.0)	6 (25.0)	12 (30.8)
PD	0	1 (100)	0	1 (4.2)	4 (10.3)
ORR (CR, CRi, or PR)	16 (84.2)	0	1 (25.0)	17 (70.8)	23 (59.0)
90% CI	(64.1–95.6)	(0–95.0)	(1.3–75.1)	(52.1–85.4)	(44.6–72.3)

The 90% CI was calculated using the exact method.

TTP events were observed, and the median TTP was not evaluable (NE; 95% CI, 26.3–NE). Twenty patients (83.3%) were censored at the date of the last adequate assessment. The Kaplan–Meier–estimated TTP rates at 6 and 12 months were consistent at 91.0% (95% CI, 68.6–97.7).

At C9D1, 17 patients (43.6%) had uMRD at the threshold of 10^{-4} in blood or bone marrow. Of the 17 patients who attained uMRD, all of them achieved it in blood. Thirteen patients (33%) had uMRD in both their bone marrow and blood, whereas four patients achieved uMRD solely in the blood. Among these 17 patients, seven patients had received ibrutinib only prior to study enrollment, and 10 patients received treatment prior to ibrutinib. Among the 17 patients who achieved uMRD at C9D1, four (23.5%) TTP events were observed. Thirteen (76.5%) patients were censored. The Kaplan–Meier–estimated (%) TTP rate (95% CI) at 6 and 12 months was 93.8% (63.2–99.1). In contrast, for the 22 patients who did not achieve uMRD at C9D1, 11 (50%) TTP events were observed, with 11 patients (50%) censored, and the estimated TTP rate was 69.2% (43.3–85.1) at 12 months. Of the 13 patients who achieved uMRD in bone marrow at C9D1, two (15.4%) TTP events were observed. Eleven (84.6%) patients were censored, and the median TTP was NE (95% CI, 26.3–NE). The ORR in these 13 patients was 92.3%, with eight (61.5%) patients achieving CR and four (30.8%) patients achieving PR.

In the full set of 39 patients, the median best percentage change from baseline up to C9D1 in blood MRD was −99.16% (range, −100.0% to −16.7%), and the median percent change from baseline to C9D1 in bone marrow was −99.98% (range, −100.0% to 1,346.3%; **Fig. 3**). Changes in the levels of CLL cells in bone marrow (as measured by flow cytometry) from baseline to C9D1, for patients with or without baseline ibrutinib resistance mutations, are displayed in Supplementary Fig. S1. From baseline to C9D1 in blood, reductions in B-cell concentrations were often observed in the first few cycles of treatment and remained at low levels through C9D1 in the ianalumab 3.0 mg/kg + ibrutinib arm patients without baseline ibrutinib resistance mutations compared with fewer reductions observed in the patients with mutations (Supplementary Fig. S2).

PK and BAFF-RO

Time course of ianalumab concentration during cycle 1 and cycle 3 and PK parameters for ianalumab are shown in Supplementary Fig. S3A and S3B and Supplementary Table S8, respectively. Ianalumab PK was largely linear across the tested doses when baseline B-cell levels were less than 10,000 cells/μL. Patients with higher baseline disease burden (baseline B-cell levels higher than 10,000 cells/μL) at lower doses had lower than expected trough concentration in the initial cycles, suggesting signs of target-mediated drug disposition.

Ianalumab total and maximal exposure (AUCtau and Cmax, respectively) did not show any major deviation from dose proportionality from 3.0 to 9.0 mg/kg at both cycle 1 and cycle 3. The variability in PK exposure at both cycles was moderate, as shown by the geometric mean coefficient of variation (ranging from 13.3% to 59.8% for Cmax and from 6.8% to 31.8% for AUCtau). There was a moderate accumulation in total systemic exposure from cycle 1 to cycle 3, ranging from 1.52- to 1.76-fold across doses. The elimination half-life ranged from 2.31 to 5.28 days at cycle 1 and from 5.04 to 6.74 days at cycle 3.

Ibrutinib PK was in line with published data in patients with CLL. Soluble BAFF in circulation has been reported to increase rapidly after dosing across ianalumab clinical studies, likely as a result of displacement from its binding to BAFF-R on B cells and loss of BAFF-R–expressing cells (41, 42). In this study, the median soluble BAFF increased two- to fivefold 2 hours after dose, similarly across doses, suggesting extensive target binding. Pooled data across all dose levels show a median fold change of 2.67, with lower and upper quartiles of 1.64 and 5.34, respectively. Peripheral BAFF-RO measurements were between 95% and 99% in >90% of samples, indicating the extensive target saturation in circulation across the tested dose range (Supplementary Fig. S4A and S4B).

Immunogenicity

Of the 39 patients, majority (36 patients, 92.3%) was ADA negative at baseline, and only three patients (7.7%) were ADA positive at baseline. None of the patients (whether ADA negative or ADA positive at baseline) had positive ADA after dose. Therefore, there were neither treatment-induced nor treatment-boosted immunogenic responses to ianalumab during the study (Supplementary Table S9). The ADA prevalence at baseline was 11.1% (three of 27) in the ianalumab 3.0 mg/kg + ibrutinib 420 mg expansion group (and 0% in the other treatment groups).

Dose determination

No DLTs were observed at any of the dose levels investigated; therefore, the MTD was not reached. The RDE was established

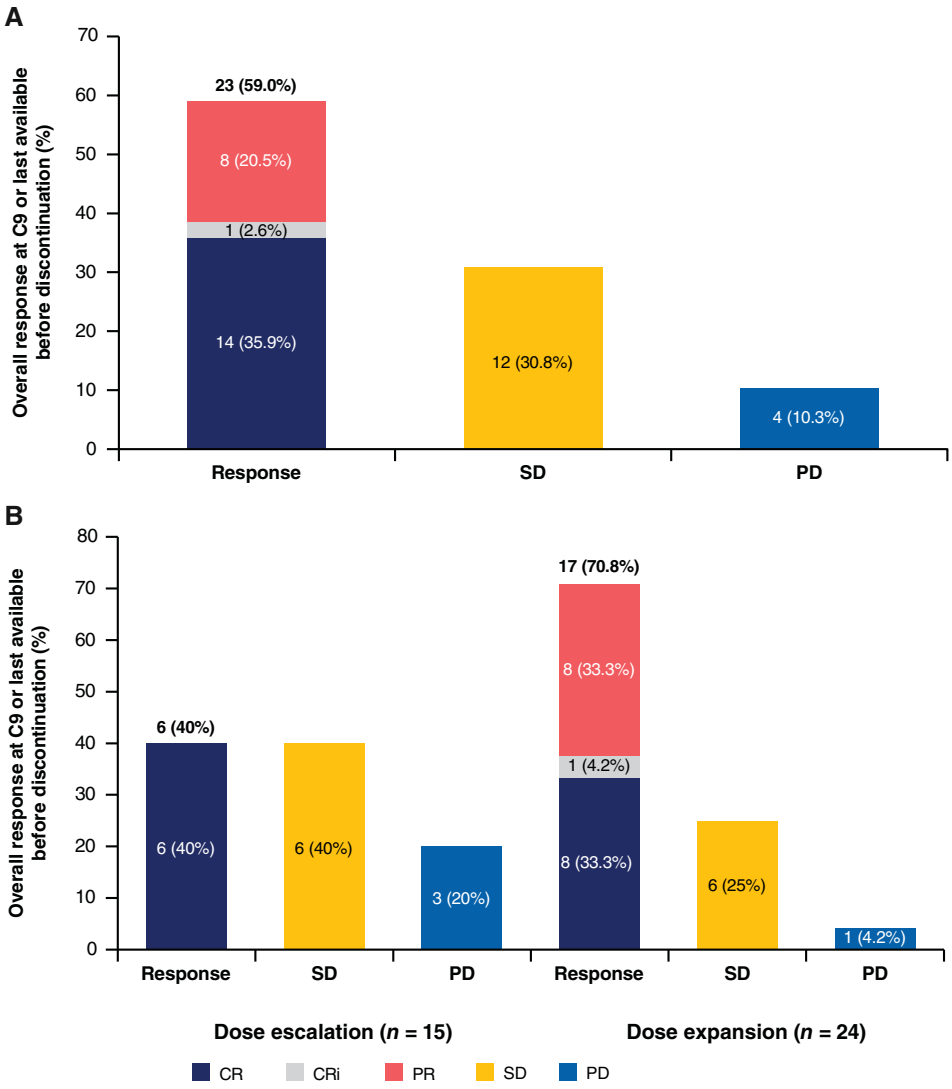

Figure 2.
Overall response at cycle 9 (C9; **A**) overall and (**B**) during dose-escalation and dose-expansion phases.

based on all available clinical data in addition to data from PK modeling. A population PK model was developed (in Monolix 2021R2) to describe the PK using a two-compartment model with linear disposition. The model predicted linear PK at doses of 3.0 mg/kg once every 2 weeks and above, as well as in patients with high tumor burden at baseline (e.g., 48, 000 cells/μL). Assuming the *in vitro* equilibrium dissociation constant of ianalumab, the serum and hypothetical disease-related tissue RO were simulated and used to estimate levels of target saturation. The serum RO was predicted to be saturated at the lowest dose of 0.3 mg/kg once every 2 weeks (Supplementary Fig. S4A). Assuming a 30% of tissue penetration (43, 44), the predicted tissue RO at steady state was >99% at 3.0 mg/kg once every 2 weeks in >95% of patients (Supplementary Fig. S4B). Therefore, integrated analysis of safety, efficacy, and PK (population PK and RO) supported the selection of an RDE of 3.0 mg/kg once every 2 weeks. At this dose, PK was anticipated to be linear independent of baseline disease burden and the target to be fully saturated both in circulation and relevant tissues. This dose showed acceptable tolerability profile and signs of clinical response.

Biomarkers

At baseline, 15 patients had *BTK* and/or *PCLγ2* mutations, with either one clone detected ($n = 9$) or between two and four clones of either mutation detected ($n = 6$); full details on baseline clones and VAFs are presented in Supplementary Table S10.

Following treatment with the combination of ianalumab and ibrutinib, the majority of patients with a *BTK* mutation at baseline whose mutation status was reevaluated at C9D1 continued to display a detectable *BTK* mutation at the end of the treatment ($n = 8/8$ with a BTK^{C481S} mutation; $n = 3/4$ with a *PCLγ2* mutation); however, in one patient with baseline *PLCγ2* mutation, detectable mutant clones were eradicated at C9D1. Nevertheless, the patient presented with the mutant clones again during evaluations at 9 and 15 months after C9D1, coinciding with relapse of the disease.

For patients with multiple clones, all baseline dominant clones (determined by the maximum VAF among all mutations) remained dominant over time; nondominant clones were excluded from subsequent analyses. The median baseline VAF for *BTK* mutations ($n = 11$) was 26.8% (range, 1.2–96.9) and for *PCLγ2* mutations

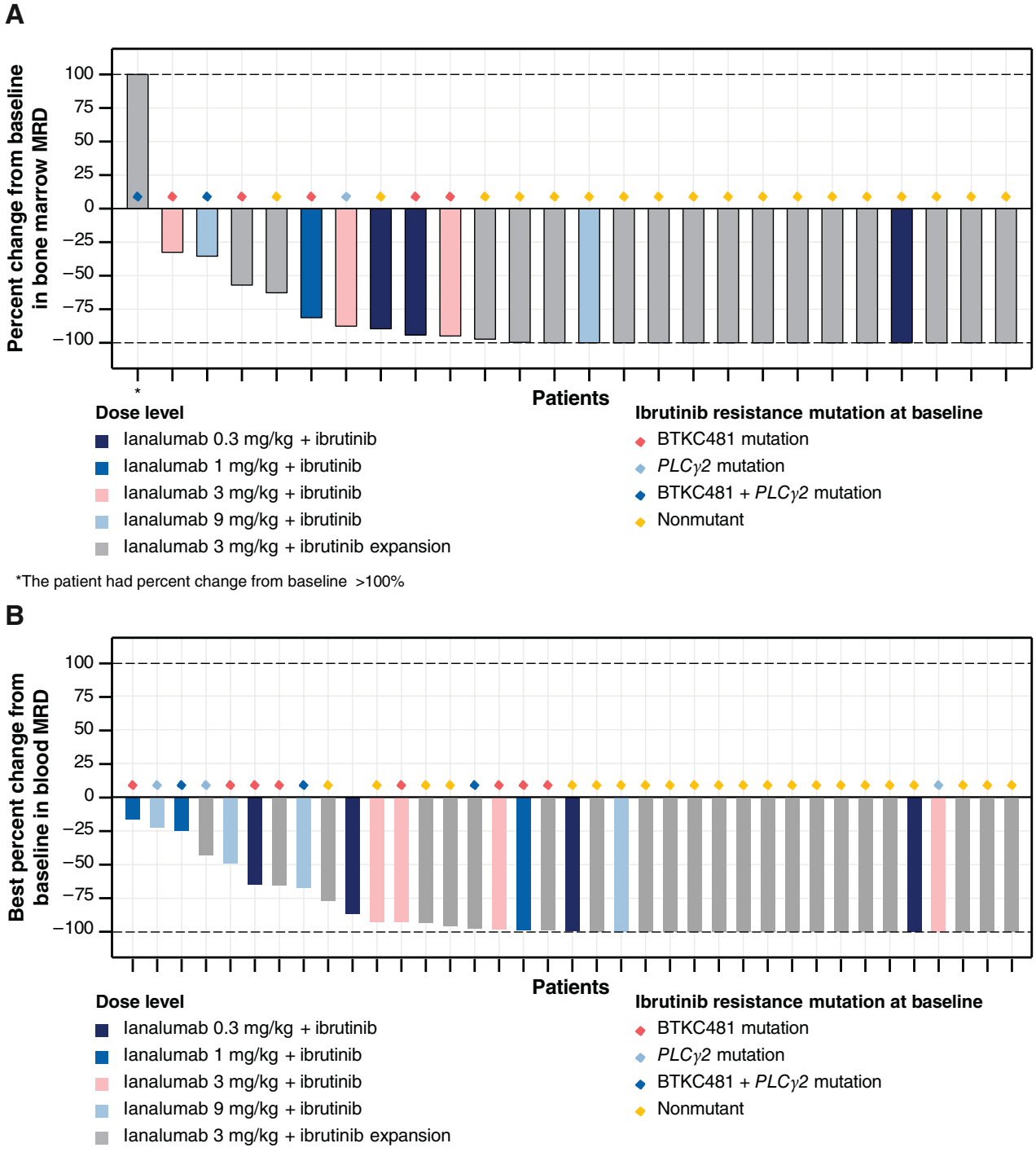

Figure 3.

Best percentage change from baseline in (**A**) bone marrow MRD and (**B**) blood MRD for individual patients in the dose-escalation and -expansion phases of the study.

($n = 7$) was 1.6% (range, 0.3–10.9). For 11 patients with at least one post-baseline VAF assessment, VAF changes for *PCLγ2* mutations tended to be stable over time, whereas VAF changes for *BTK* mutations exhibited heterogeneity, with VAF increases in four of nine patients at or prior to the time of progression (Supplementary Fig. S5).

PBMC analysis

PBMCs from patients treated with ianalumab (3.0 mg/kg) were analyzed by flow cytometry to determine levels of activated NK cells (NKp46-positive and NKG2D-expressing NK cells; Supplementary Fig. S6). At C1D1, 1 hour after dose, the frequency of peripheral NKp46-positive NK cells increased at least 50% after ianalumab

3 mg/kg treatment in approximately half of the patients compared with C1D1 before dose. Patients in SD tended to show no or little change in NKp46 at 1 hour after dose or at day 2 before dose, whereas patients in CR and PR tended to show increases at 1 hour after dose or day 2 before dose. Baseline counts of NK cells and NKG2D-expressing NK cells in the blood were higher in responders than in nonresponders (Supplementary Fig. S7). It should be noted that sample sizes are small, so only trends can be observed in these data.

RNA-seq

Preliminary coverage-based limiting-cell experiment analysis for RNA-seq (CLEAR) data from 14 patients supports peripheral NK- and T-cell activation with ianalumab. At C1D1, 1 hour after dose, RNA-seq analysis showed an increase in effector-related gene expression in NK cells (*ETS1*, *KLRD1*, *ISG20*, and *PRF1*; Supplementary Fig. S8A), in $CD8^+$ T cells (*ETS1*, *CD53*, *ISG20*, and *PRF1*; Supplementary Fig. S8B), and in $CD4^+$ T cells (*IL6ST*, *ADAM10*, *BIRC3*, *ITK*, and *CASP6*; Supplementary Fig. S8C) with ianalumab treatment, suggesting increased effector function of these cells. RNA-seq analysis showed evidence of apoptosis induction–related gene expression (*TP53INP1* and apoptosis-related gene signature) in CLL cells (Supplementary Fig. S9A and S9B).

Antibody levels in the blood were also measured at baseline and on treatment. Overall, IgA, IgG, and IgM levels did not significantly drop following initial treatment, and those levels were maintained over the course of treatment (Supplementary Fig. S10).

Discussion

The ianalumab and ibrutinib combination was well tolerated, seemed active, and had an acceptable safety profile, enabling dose expansion.

Ianalumab exposure did not show any major deviation from dose proportionality from 3.0 to 9.0 mg/kg. There was extensive target saturation in circulation across tested doses. Based on PK data and modeling, along with biomarker data, clinical safety, and efficacy, the RDE was established as 3.0 mg/kg once every 2 weeks.

The long-term persistent detectable MRD has significant implications for patients as they are required to continue ibrutinib treatment in the setting of persistent detectable MRD to maintain disease control. In this study, 43.6% of patients attained uMRD status in blood or bone marrow, which is a sufficiently deep response to discontinue treatment. CR with or without complete bone marrow recovery was numerically more common among patients in the expansion phase who were receiving first-line ibrutinib at the time of study enrollment. There is a potential for discontinuation of ibrutinib after uMRD has been achieved, allowing for the avoidance of toxicity that may occur because of the indefinite therapy of BTKi. The rate of achieving uMRD seen in the study is comparable with other similar studies in patients with CLL, in which another therapy is added to ibrutinib (45–47). Patients receiving BTKi are immunocompromised and are at risk of infections (48). In this study, the infection rate seemed to be lower in patients treated with ianalumab and ibrutinib (46.2%, any-grade infection and no grade ≥3 infections reported) compared with those treated with single-agent BTKi (≥70% for any grade and ≥24% for grade ≥3 infections; refs. 49, 50). The data suggest that the addition of ianalumab to ibrutinib did not increase the infection rates. Overall, the safety profile of ianalumab added to ibrutinib is well tolerated and aligns with findings from other studies in which additional therapies are added to ibrutinib in patients with CLL (45–47).

A major limitation of ibrutinib therapy is the potential that ibrutinib resistance mutations may occur such as BTK^{C481S}, which eliminates covalent binding and also greatly decreases the affinity of ibrutinib for BTK and ability to inhibit BTK activation of downstream target *PLCγ2* (26). Resistance to treatment increases the risk that disease progression will occur in the future. Most patients enrolled in this study are BTK^{C481S}/*PLCγ2* wild type; thus, conclusions related to how baseline BTK mutations influenced treatment outcomes or how mutation status altered the treatment cannot be drawn. Furthermore, another limitation of the study is lack of longer-term follow-up of the patients, leaving uncertainty on how viable a discontinuation strategy will be.

ADCC is primarily exerted by NK cells, and we demonstrate evidence of NK-cell activation with treatment in this study. RNA-seq data suggested increased activation of effector function in NK cells and T cells. The NK cell–mediated ADCC is also involved in other CD20 antibodies, including rituximab (51, 52). Patients who responded to treatment tended to have acute increases in activated NK, suggesting that effective ianalumab treatment increases NK-cell activation, likely because of positive feedback mechanisms through non–cell-autonomous activation (e.g., cytokines). In addition, responders tended to have higher levels of NK cells and activated NK cells at baseline. These data together support the proposed mechanism of action of ADCC-mediated killing of tumor cells by NK cells. T-cell activation in the context of an ADCC antibody occurs either via cytokine secretion from activated NK cells or is directly mediated through binding to CD16 expressed on $CD8^+$ T cell (53, 54) in agreement with our RNA-seq data in pre- and post-ianalumab treatment. Therefore, the antileukemia activity of ianalumab likely is exerted through multiple immune-mediated effects, such as by ADCC-mediated killing from NK and T cells. However, given that this was a novel and exploratory analysis, we did not collect subsequent samples to perform further analysis. A larger study is warranted to correlate T-cell activation with a response. RNA-seq data also demonstrated evidence of apoptosis induction in CLL cells following initial treatment with ianalumab. The mechanism of apoptosis induction on CLL cells cannot be confirmed with the current methods, as CLL cells could experience apoptosis either as a result of cytotoxic activity from NK or T cells or through blockade of BAFF ligand binding to BAFF-R and subsequent decrease in NF-κB signaling (18).

Addition of ianalumab to covalent BTKi in the treatment of CLL holds potential. The combination could offer a safer therapeutic option with improved selectivity and reduced side effects and possibly allow some patients to discontinue BTKi after achieving uMRD, resulting in shorter treatment duration and lower toxicity. As combination therapy with BTKi for fixed durations is being increasingly utilized and data from other studies show that antibodies such as obinutuzumab can improve PFS (12), a strategy of adding ianalumab to ibrutinib could be beneficial in deepening disease responses and improving PFS or allowing patients to stop BTKi therapy with minimal toxicity. Although this study was done with ibrutinib, based on the mechanism, we would expect the same results with other covalent BTKi that are now more recommended because of improved cardiovascular toxicities.

In this phase Ib study, the combination of ianalumab and ibrutinib was well tolerated and resulted in almost half the patients achieving uMRD status in blood or bone marrow. The present results suggest that adding ianalumab to ibrutinib for the treatment of

patients with CLL may be a viable strategy to reduce the duration of BTKi therapy. However, a larger study is necessary to confirm this therapeutic hypothesis.

Data Availability

Data are available upon reasonable request. Novartis will not provide access to patient-level data if there is a reasonable likelihood that individual patients could be re-identified. Phase I studies, by their nature, present a high risk of patient reidentification; therefore, patient individual results for phase I studies cannot be shared. In addition, clinical data, in some cases, have been collected subject to contractual or consent provisions that prohibit transfer to third parties. Such restrictions may preclude granting access under these provisions. Where co-development agreements or other legal restrictions prevent companies from sharing particular data, companies will work with qualified requestors to provide summary information where possible.

Authors' Disclosures

K.A. Rogers reports grants from Novartis during the conduct of the study, as well as grants and personal fees from AbbVie, Genentech, AstraZeneca, and Loxo@Lilly and personal fees from Janssen Pharmaceuticals, BeiGene, Pharmacyclics, and Alpine Immune Sciences outside the submitted work. I.W. Flinn reports personal fees from AbbVie, BeiGene, Genentech, Genmab, Kite Pharma, and Vincerx Pharma and grants from AbbVie, AstraZeneca, BeiGene, Bristol Myers Squibb, Celgene, City of Hope National Medical Center, Epizyme, Fate Therapeutics, Genentech, Gilead Sciences, IGM Biosciences, InnoCare Pharma, Incyte, Janssen Pharmaceuticals, Kite Pharma, Loxo Oncology, Marker Therapeutics, Merck, MorphoSys, Myeloid Therapeutics, Novartis, Nurix, Pfizer, Roche, Seattle Genetics, TG Therapeutics, Vincerx Pharma, and 270 Bio during the conduct of the study. D.M. Stephens reports grants from Novartis during the conduct of the study, as well as grants and personal fees from AbbVie, AstraZeneca, BeiGene, Bristol Myers Squibb, and Genentech and personal fees from Eli Lilly and Company, Johnson & Johnson, and Pharmacyclics outside the submitted work. S.M. Larson reports grants from Allogene, Bristol Myers Squibb, Janssen Pharmaceuticals, Regeneron Therapeutics, Kite Pharma, Pfizer, and Sanofi outside the submitted work. L. Martz reports grants from Novartis during the conduct of the study. R. Sechaud reports ownership of Novartis stock and employment with Novartis. D. Baldoni reports employment with Novartis and ownership of Novartis shares. N.B. Hassounah reports a patent for Treatment of B-Cell Malignancies (CA3190678A1) pending and a patent for Treatment of CLL (US20230340136A1) pending, as well as ownership of Novartis stock. N. Orwitz reports employment with Novartis. J. Otero reports other support from Novartis during the conduct of the study, as well as other support from Novartis outside the submitted work. J. Woo reports other support from Novartis during the conduct of the study, as well as grants from Sobi and PROTEINA outside the submitted work. No disclosures were reported by the other authors.

Authors' Contributions

K.A. Rogers: Supervision, visualization, methodology, writing–original draft, writing–review and editing. **P. Yan:** Writing–original draft, writing–review and editing. **I.W. Flinn:** Writing–original draft, writing–review and editing. **D.M. Stephens:** Writing–original draft, writing–review and editing. **T.J. Kipps:** Writing–original draft, writing–review and editing. **S.M. Larson:** Writing–original draft, writing–review and editing. **L. Martz:** Writing–original draft, writing–review and editing. **X. Chen:** Writing–original draft, writing–review and editing. **H. Wang:** Writing–original draft, writing–review and editing. **E. Hopping:** Writing–original draft, writing–review and editing. **R. Bundschuh:** Writing–original draft, writing–review and editing. **A. Turkoglu:** Writing–original draft, writing–review and editing. **G. Lozanski:** Writing–original draft, writing–review and editing. **C. McGarry:** Writing–original draft, writing–review and editing. **A. Acosta:** Writing–original draft, writing–review and editing. **R. Sechaud:** Writing–original draft, writing–review and editing. **D. Baldoni:** Writing–original draft, writing–review and editing. **A. Chaudhury:** Writing–original draft, writing–review and editing. **J. Whalen:** Writing–original draft, writing–review and editing. **N.B. Hassounah:** Formal analysis, writing–original draft, writing–review and editing. **N. Orwitz:** Data curation, formal analysis, validation, methodology, writing–original draft, writing–review and editing. **J. Otero:** Writing–original draft, writing–review and editing. **J. Woo:** Writing–original draft, writing–review and editing. **J.C. Byrd:** Writing–original draft, writing–review and editing.

Acknowledgments

We thank Tanya Mulvey and David Quinn for assistance with flow cytometry methods and members of Navigate BioPharma Services Kimberley-Jane Bonjoc, Nadia Katkova, and Keith Kwak for flow cytometry sample analyses. We would also like to thank Daniel Jones, Rachel Hess, and Nehad Mohamed for ibrutinib resistance mutation data and bioinformatic analysis and Susan Long and the staff and directors of the Polaris Molecular Laboratory for sequence analysis. We also thank Bethany Mundy-Bosse for her contribution to the NK-cell studies. In addition, we would like to thank Rhonda Kitzler and Rebecca Pearson for providing MRD data. KAR is a scholar in clinical research of the Leukemia and Lymphoma Society (CDP 2331-20). Swati Machwe, PhD, of Novartis Healthcare Pvt Ltd. provided medical writing assistance. This study was funded by Novartis Pharmaceuticals Corporation, which also provided funding for medical writing assistance.

Note

Supplementary data for this article are available at Clinical Cancer Research Online (http://clincancerres.aacrjournals.org/).

Received January 27, 2025; revised May 9, 2025; accepted September 22, 2025; posted first November 6, 2025.

References

1. Burger JA. Bruton tyrosine kinase inhibitors: present and future. Cancer J 2019;25:386–93.
2. U.S. Food and Drug Administration. FDA grants accelerated approval to pirtobrutinib for chronic lymphocytic leukemia and small lymphocytic lymphoma. U.S. Food and Drug Administration; 2023 [cited 2025 Jul 29]. Available from: https://www.fda.gov/drugs/resources-information-approved-drugs/fda-grants-accelerated-approval-pirtobrutinib-chronic-lymphocytic-leukemia-and-small-lymphocytic.
3. Frustaci AM, Deodato M, Zamprogna G, Cairoli R, Montillo M, Tedeschi A. Next generation BTK inhibitors in CLL: evolving challenges and new opportunities. Cancers (Basel) 2023;15:1504.
4. Lipsky A, Lamanna N. Managing toxicities of Bruton tyrosine kinase inhibitors. Hematol Am Soc Hematol Educ Program 2020;2020:336–45.
5. Mato AR, Nabhan C, Thompson MC, Lamanna N, Brander DM, Hill B, et al. Toxicities and outcomes of 616 ibrutinib-treated patients in the United States: a real-world analysis. Haematologica 2018;103:874–9.
6. Maddocks KJ, Ruppert AS, Lozanski G, Heerema NA, Zhao W, Abruzzo L, et al. Etiology of ibrutinib therapy discontinuation and outcomes in patients with chronic lymphocytic leukemia. JAMA Oncol 2015;1:80–7.
7. Ahn IE, Underbayev C, Albitar A, Herman SEM, Tian X, Maric I, et al. Clonal evolution leading to ibrutinib resistance in chronic lymphocytic leukemia. Blood 2017;129:1469–79.
8. Kadri S, Lee J, Fitzpatrick C, Galanina N, Sukhanova M, Venkataraman G, et al. Clonal evolution underlying leukemia progression and Richter transformation in patients with ibrutinib-relapsed CLL. Blood Adv 2017;1:715–27.
9. Woyach JA, Ruppert AS, Guinn D, Lehman A, Blachly JS, Lozanski A, et al. BTK^{C481S}-mediated resistance to ibrutinib in chronic lymphocytic leukemia. J Clin Oncol 2017;35:1437–43.
10. Chirino A, Montoya S, Safronenka A, Taylor J. Resisting the resistance: navigating BTK mutations in chronic lymphocytic leukemia (CLL). Genes (Basel) 2023;14:2182.
11. Woyach JA, Ruppert AS, Mandrekar SJ. Ibrutinib regimens in older patients with untreated CLL. Reply. N Engl J Med 2019;380:1680–1.
12. Sharman JP, Egyed M, Jurczak W, Skarbnik A, Pagel JM, Flinn IW, et al. Efficacy and safety in a 4-year follow-up of the ELEVATE-TN study comparing acalabrutinib with or without obinutuzumab versus obinutuzumab plus chlorambucil in treatment-naïve chronic lymphocytic leukemia. Leukemia 2022;36:1171–5.

13. Shanafelt TD, Wang XV, Kay NE, Hanson CA, O'Brien S, Barrientos J, et al. Ibrutinib-rituximab or chemoimmunotherapy for chronic lymphocytic leukemia. N Engl J Med 2019;381:432–43.
14. Moreno C, Greil R, Demirkan F, Tedeschi A, Anz B, Larratt L, et al. Ibrutinib plus obinutuzumab versus chlorambucil plus obinutuzumab in first-line treatment of chronic lymphocytic leukaemia (iLLUMINATE): a multicentre, randomised, open-label, phase 3 trial. Lancet Oncol 2019;20:43–56.
15. Schneider P, MacKay F, Steiner V, Hofmann K, Bodmer JL, Holler N, et al. BAFF, a novel ligand of the tumor necrosis factor family, stimulates B cell growth. J Exp Med 1999;189:1747–56.
16. Rodig SJ, Shahsafaei A, Li B, Mackay CR, Dorfman DM. BAFF-R, the major B cell-activating factor receptor, is expressed on most mature B cells and B-cell lymphoproliferative disorders. Hum Pathol 2005;36:1113–9.
17. Jasek M, Bojarska-Junak A, Wagner M, Sobczyński M, Wołowiec D, Roliński J, et al. Association of variants in BAFF (rs9514828 and rs1041569) and BAFF-R (rs61756766) genes with the risk of chronic lymphocytic leukemia. Tumour Biol 2016;37:13617–26.
18. McWilliams EM, Lucas CR, Chen T, Harrington BK, Wasmuth R, Campbell A, et al. Anti-BAFF-R antibody VAY-736 demonstrates promising preclinical activity in CLL and enhances effectiveness of ibrutinib. Blood Adv 2019;3:447–60.
19. Dörner T, Posch M, Wagner F, Hüser A, Fischer T, Mooney L, et al. THU0313 double-blind, randomized study of VAY736 single dose treatment in patients with primary Sjögren's syndrome (PSS). Ann Rheum Dis 2016;75(Suppl 2):300–1.
20. Claudio E, Brown K, Park S, Wang H, Siebenlist U. BAFF-induced NEMO-independent processing of NF-kappa B2 in maturing B cells. Nat Immunol 2002;3:958–65.
21. Gardam S, Sierro F, Basten A, Mackay F, Brink R. TRAF2 and TRAF3 signal adapters act cooperatively to control the maturation and survival signals delivered to B cells by the BAFF receptor. Immunity 2008;28:391–401.
22. van Gent R, Kater AP, Otto SA, Jaspers A, Borghans JAM, Vrisekoop N, et al. In vivo dynamics of stable chronic lymphocytic leukemia inversely correlate with somatic hypermutation levels and suggest no major leukemic turnover in bone marrow. Cancer Res 2008;68:10137–44.
23. Mihalcik SA, Tschumper RC, Jelinek DF. Transcriptional and post-transcriptional mechanisms of BAFF-receptor dysregulation in human B lineage malignancies. Cell Cycle 2010;9:4884–92.
24. Hallek M, Cheson BD, Catovsky D, Caligaris-Cappio F, Dighiero G, Döhner H, et al. iwCLL guidelines for diagnosis, indications for treatment, response assessment, and supportive management of CLL. Blood 2018;131:2745–60.
25. Swerdlow SH, Campo E, Pileri SA, Harris NL, Stein H, Siebert R, et al. The 2016 revision of the World Health Organization classification of lymphoid neoplasms. Blood 2016;127:2375–90.
26. Woyach JA, Furman RR, Liu T-M, Ozer HG, Zapatka M, Ruppert AS, et al. Resistance mechanisms for the Bruton's tyrosine kinase inhibitor ibrutinib. N Engl J Med 2014;370:2286–94.
27. Jones D, Woyach JA, Zhao W, Caruthers S, Tu H, Coleman J, et al. PLCG2 C2 domain mutations co-occur with BTK and PLCG2 resistance mutations in chronic lymphocytic leukemia undergoing ibrutinib treatment. Leukemia 2017;31:1645–7.
28. Rawstron AC, Fazi C, Agathangelidis A, Villamor N, Letestu R, Nomdedeu J, et al. A complementary role of multiparameter flow cytometry and high-throughput sequencing for minimal residual disease detection in chronic lymphocytic leukemia: an European Research Initiative on CLL study. Leukemia 2016;30:929–36.
29. Rawstron AC, Villamor N, Ritgen M, Böttcher S, Ghia P, Zehnder JL, et al. International standardized approach for flow cytometric residual disease monitoring in chronic lymphocytic leukaemia. Leukemia 2007;21:956–64.
30. Conlon K, Watson DC, Waldmann TA, Valentin A, Bergamaschi C, Felber BK, et al. Phase I study of single agent NIZ985, a recombinant heterodimeric IL-15 agonist, in adult patients with metastatic or unresectable solid tumors. J Immunother Cancer 2021;9:e003388.
31. Schubert M, Lindgreen S, Orlando L. AdapterRemoval v2: rapid adapter trimming, identification, and read merging. BMC Res Notes 2016;9:88.
32. Kim D, Langmead B, Salzberg SL. HISAT: a fast spliced aligner with low memory requirements. Nat Methods 2015;12:357–60.
33. O'Leary NA, Wright MW, Brister JR, Ciufo S, Haddad D, McVeigh R, et al. Reference sequence (RefSeq) database at NCBI: current status, taxonomic expansion, and functional annotation. Nucleic Acids Res 2016;44:D733–45.
34. Liao Y, Smyth GK, Shi W. The Subread aligner: fast, accurate and scalable read mapping by seed-and-vote. Nucleic Acids Res 2013;41:e108.
35. Liao Y, Smyth GK, Shi W. featureCounts: an efficient general purpose program for assigning sequence reads to genomic features. Bioinformatics 2014;30:923–30.
36. Kroll KW, Mokaram NE, Pelletier AR, Frankhouser DE, Westphal MS, Stump PA, et al. Quality control for RNA-seq (QuaCRS): an integrated quality control pipeline. Cancer Inform 2014;13(Suppl 3):7–14.
37. DeLuca DS, Levin JZ, Sivachenko A, Fennell T, Nazaire M-D, Williams C, et al. RNA-SeQC: RNA-seq metrics for quality control and process optimization. Bioinformatics 2012;28:1530–2.
38. Wang L, Wang S, Li W. RSeQC: quality control of RNA-seq experiments. Bioinformatics 2012;28:2184–5.
39. Quinlan AR, Hall IM. BEDTools: a flexible suite of utilities for comparing genomic features. Bioinformatics 2010;26:841–2.
40. Walker LA, Sovic MG, Chiang C-L, Hu E, Denninger JK, Chen X, et al. CLEAR: coverage-based limiting-cell experiment analysis for RNA-seq. J Transl Med 2020;18:63.
41. Dörner T, Posch MG, Li Y, Petricoul O, Cabanski M, Milojevic JM, et al. Treatment of primary Sjögren's syndrome with ianalumab (VAY736) targeting B cells by BAFF receptor blockade coupled with enhanced, antibody-dependent cellular cytotoxicity. Ann Rheum Dis 2019;78:641–7.
42. Bowman SJ, Fox R, Dörner T, Mariette X, Papas A, Grader-Beck T, et al. Safety and efficacy of subcutaneous ianalumab (VAY736) in patients with primary Sjögren's syndrome: a randomised, double-blind, placebo-controlled, phase 2b dose-finding trial. Lancet 2022;399:161–71.
43. Shemesh CS, Chanu P, Jamsen K, Wada R, Rossato G, Donaldson F, et al. Population pharmacokinetics, exposure-safety, and immunogenicity of atezolizumab in pediatric and young adult patients with cancer. J Immunother Cancer 2019;7:314.
44. Deng R, Bumbaca D, Pastuskovas CV, Boswell CA, West D, Cowan KJ, et al. Preclinical pharmacokinetics, pharmacodynamics, tissue distribution, and tumor penetration of anti-PD-L1 monoclonal antibody, an immune checkpoint inhibitor. MAbs 2016;8:593–603.
45. Thompson PA, Keating MJ, Ferrajoli A, Jain N, Peterson CB, Garg N, et al. Venetoclax consolidation in high-risk CLL treated with ibrutinib for ≥1 year achieves a high rate of undetectable MRD. Leukemia 2023;37:1444–53.
46. Rogers KA, McLaughlin E, Wei L, Bhat SA, Crouse A, Grever MR, et al. Initial results of a phase 2 study of venetoclax added to ibrutinib to eliminate ibrutinib resistance mutations in CLL. Blood 2023;142(Suppl 1):1899.
47. Roeker LE, Feldman TA, Soumerai JD, Falco V, Panton G, Dorsey C, et al. Adding umbralisib and ublituximab (U2) to ibrutinib in patients with CLL: a phase II study of an MRD-driven approach. Clin Cancer Res 2022;28:3958–64.
48. Palma M, Mulder TA, Österborg A. BTK inhibitors in chronic lymphocytic leukemia: biological activity and immune effects. Front Immunol 2021;12:686768.
49. Byrd JC, Brown JR, O'Brien S, Barrientos JC, Kay NE, Reddy NM, et al. Ibrutinib versus ofatumumab in previously treated chronic lymphoid leukemia. N Engl J Med 2014;371:213–23.
50. Coutre SE, Byrd JC, Hillmen P, Barrientos JC, Barr PM, Devereux S, et al. Long-term safety of single-agent ibrutinib in patients with chronic lymphocytic leukemia in 3 pivotal studies. Blood Adv 2019;3:1799–807.
51. Enqvist M, Jacobs B, Junlén HR, Schaffer M, Melén CM, Friberg D, et al. Systemic and intra-nodal activation of NK cells after rituximab monotherapy for follicular lymphoma. Front Immunol 2019;10:2085.
52. Veeramani S, Wang S-Y, Dahle C, Blackwell S, Jacobus L, Knutson T, et al. Rituximab infusion induces NK activation in lymphoma patients with the high-affinity CD16 polymorphism. Blood 2011;118:3347–9.
53. Björkström NK, Gonzalez VD, Malmberg K-J, Falconer K, Alaeus A, Nowak G, et al. Elevated numbers of Fc gamma RIIIA+ ($CD16^+$) effector CD8 T cells with NK cell-like function in chronic hepatitis C virus infection. J Immunol 2008;181:4219–28.
54. Rosenberg J, Huang J. $CD8^+$ T cells and NK cells: parallel and complementary soldiers of immunotherapy. Curr Opin Chem Eng 2018;19:9–20.